Grzegorz TARCHAŁA, Teresa ORŁOWSKA-KOWALSKA, Khanh NGUYEN-THAC, Mateusz DYBKOWSKI

Wrocław University of Technology, Institute of Electrical Machines, Drives and Measurements

Performance analysis of the sensorless direct torque controlled induction motor drive with optimal field weakening algorithm in traction applications

Abstract. *The paper deals with a sensorless induction motor drive operating in the field weakening region, intended for traction application. Optimal field weakening algorithm takes into consideration stator current and voltage constraints. The direct torque control with space vector modulation DTC-SVM method is applied to control the drive. Angular speed of the induction motor is estimated using two adaptive estimators with reference model.*

Streszczenie. *W artykule przedstawiony został bezczujnikowy napęd indukcyjny pracujący w zakresie osłabiania pola, przeznaczony do zastosowań trakcyjnych. Optymalny algorytm osłabiania pola uwzględnia ograniczenia amplitud prądu i napięcia stojana. Napęd sterowany jest przy użyciu metody bezpośredniego sterowania momentem, z modulatorem wektorowym DTC-SVM. Prędkość kątowa silnika estymowana jest za pomocą dwóch estymatorów z modelem odniesienia.(**Analiza właściwości bezczujnikowego układu napędowego z optymalnym algorytmem osłabiania pola w zastosowaniach trakcyjnych**)*

Keywords: induction motor, traction drive, field weakening, speed estimation.
Słowa kluczowe: silnik indukcyjny, napęd trakcyjny, osłabianie pola, estymacja prędkości.

Introduction

Application of induction motors in traction drive systems allows to lower the costs and increase the operational reliability of such drives [1]. In order to ensure the motor torque ideal control, the field-oriented control structures have to be applied. In modern solutions the most popular method is the Direct Torque Control with Space Vector Modulation (DTC-SVM). The use of the modulator ensures constant switching frequency of the voltage inverter transistors, on the contrary to the classical Direct Torque Control with the switching table [2].

In traction drives there is no outer speed regulator – tram driver takes over this function. In spite of this, in the majority of nowadays traction drives, speed is estimated in diagnostic purposes with use of the incremental encoder. However, this sensor often gets damaged, for instance because of the road unevenness. In order to increase the reliability of the drive in case of the encoder failure, the simultaneous speed estimation is proposed.

There exist many various induction motor speed estimation methods [1]. One of the simplest and the most certain estimation method are Model Reference Adaptive System (MRAS) estimators [3], [4]. There are a few basic solutions of this kind of estimators [5], depending on the reference and adaptive models and adaptation mechanism. In this paper two different solutions will be presented, both using the current model in rotor flux estimation and the stator current dynamical equation as the adaptive models. The induction motor is the reference system. Presented estimators utilize two different adaptation mechanisms: Pi regulator [5] in the MRAS^{CC} estimator, and the sign function in SM-MRAS estimator [6]. Both estimators were compared in [7]. Systems of this type show bigger insensitivity over motor parameters changes, on the contrary to other solutions [8],[9].

High speed operation (even twice the nominal speed value) is required in traction drives. With regard to the available voltage limitation and current constraint (to protect the stator winding and power electronics), there is a necessity to weaken the flux of the machine. In such operation condition the maximal available torque decreases, too. The simplest solution of the field-weakening is to decrease the reference flux amplitude inverse proportionally to the motor speed.

However, this method is not optimal with respect to the available voltage and taking into consideration the current constraint [10]-[12]. Another important issue is the field weakening algorithm to respond to the DC voltage changes, frequent during the traction drive operation.

In the paper the optimal field weakening algorithm is used for sensorless induction motor traction drive, working in very wide speed range. The described problems are illustrated using both simulation and experimental results obtained for the 50 kW induction motor drive.

Mathematical model of the induction machine

Mathematical model of 3-phase squirrel cage induction motor can be described using vector equations in a coordinate frame rotating with any velocity ω_k using commonly known simplifications (such as construction symmetry, windings symmetry, air gap uniformity, no eddy currents) with the following relationships [1]:

— stator and rotor voltage equations:

$$\mathbf{u_s} = r_s \mathbf{i_s} + T_N \frac{d}{dt}\boldsymbol{\psi}_\mathbf{s} + j\omega_k \boldsymbol{\psi}_\mathbf{s} \tag{1}$$

$$\mathbf{0} = r_r \mathbf{i_r} + T_N \frac{d}{dt}\boldsymbol{\psi}_\mathbf{r} + j(\omega_k - \omega_m)\boldsymbol{\psi}_\mathbf{r} \tag{2}$$

— flux-current equations:

$$\boldsymbol{\psi}_\mathbf{s} = x_s \mathbf{i_s} + x_M \mathbf{i_r} \tag{3}$$

$$\boldsymbol{\psi}_\mathbf{r} = x_r \mathbf{i_r} + x_M \mathbf{i_s} \tag{4}$$

— equation of motion and motor torque equations:

$$\frac{d\omega_m}{dt} = \frac{1}{T_M}(m_e - m_o) \tag{5}$$

$$m_e = \mathrm{Im}\left(\boldsymbol{\psi}_\mathbf{s}^* \mathbf{i_s}\right) \tag{6}$$

where: $\mathbf{u_s}=u_{su}+ju_{sv}$, $\mathbf{i_s}=i_{su}+ji_{sv}$, $\mathbf{i_r}=i_{ru}+ji_{rv}$, $\boldsymbol{\psi}_\mathbf{s}=\psi_{su}+j\psi_{sv}$, $\boldsymbol{\psi}_\mathbf{r}=\psi_{ru}+j\psi_{rv}$, – stator voltage and current, rotor current, stator and rotor flux vectors, motor parameters: r_s, r_r, x_M, x_s, x_r – stator and rotor resistances, magnetizing, stator and rotor reactances, shaft velocity – ω_m, torques:

electromagnetic m_e – and load m_o, constants: mechanical T_M and T_N – the effect of the per unit values introduction [1].

Thus, the induction motor equations are different for each assumed coordinate system (rotating velocity ω_k.). In this publication three different coordinate systems will be considered – first of them will be the system stationary towards the motor stator, ω_k=0. This system will be used during the speed estimator designing. The dynamical equation of the stator current vector is as follows:

$$T_N \frac{d\mathbf{i_s}}{dt} = \frac{1}{x_s \sigma}\left(\mathbf{u_s} - r_s \mathbf{i_s} - \frac{r_r x_M^2}{x_r^2}\mathbf{i_s} + \frac{x_M}{x_r}\frac{r_r}{x_r}\boldsymbol{\psi}_\mathbf{r} - j\frac{x_M}{x_r}\omega_m \boldsymbol{\psi}_\mathbf{r}\right), \tag{7}$$

where $\sigma = 1 - x_M^2 / (x_s x_r)$.

Rotor flux vector can be calculated as:

$$T_N \frac{d\boldsymbol{\psi}_\mathbf{r}}{dt} = -\frac{r_r}{x_r}\boldsymbol{\psi}_\mathbf{r} + \frac{x_M r_r}{x_r}\mathbf{i_s} + j\omega_m \boldsymbol{\psi}_\mathbf{r}. \tag{8}$$

Second coordinate frame, used in this paper will the system rotating with stator flux velocity, $\omega_k = \omega_{\psi s}$, $\psi_{sx} = \psi_s$, ψ_{sy}=0. In this system the DTC-SVM method will be defined. Stator voltage vector components in this system are as follows (1):

$$u_{sx} = r_s i_{sx} + T_N \frac{d\psi_s}{dt} \tag{9}$$

$$u_{sy} = r_s i_{sy} + \omega_{\psi s}\psi_s \tag{10}$$

Torque equation (6) in this coordinate system, with $\omega_{\psi s}\psi_s$ decoupled:

$$m_e = \psi_{sx} i_{sy} - \psi_{sy} i_{sx} \xrightarrow[\omega_{\psi s}\psi_s \text{ decoupled}]{\psi_{sx}=\psi_s,\ \psi_{sy}=0} m_e = \frac{1}{r_s}\psi_s u_{sy} \tag{11}$$

Third coordinate system is the system rotating with rotor flux vector, $\omega_k = \omega_{\psi r}$, $\psi_{rx} = \psi_r$, $\psi_{ry} = 0$. The optimal field weakening algorithm will be defined using this system. Rotor and stator flux vectors velocities are equal to the synchronous speed in a steady state, $\omega_k = \omega_s = \omega_{\psi s} = \omega_{\psi r}$.

Stator voltage vector components can be calculated in the steady state as [11]:

$$u_{sx} = r_s i_{sx} - \omega_s \sigma x_s i_{sy} \tag{12}$$

$$u_{sy} = r_s i_{sy} + \omega_s x_s i_{sx} \tag{13}$$

These equation are used in the development of the optimal field weakening (FW) algorithms.

Direct Torque Control Method using Space Vector Modulation

Direct Torque Control with Space Vector Modulation DTC-SVM, used for the induction motor drive control, can be classified to the constant flux control methods [2]. In this case stator flux amplitude is stabilized. It can be estimated from:

$$\hat{\boldsymbol{\psi}}_\mathbf{s} = x_M / x_r \hat{\boldsymbol{\psi}}_\mathbf{r} + x_s \sigma \mathbf{i_s} \tag{14}$$

Motor torque is the value, which have to be controlled ideally in the traction application. It can be estimated using the following formula, defined in the stationary reference frame:

$$\hat{m}_e = \hat{\psi}_{s\beta} i_{s\alpha} - \hat{\psi}_{s\alpha} i_{s\beta} \tag{15}$$

The principle of operation of the described control method is based on the analysis of the induction motor equations written in the coordinate system rotating with the stator flux vector velocity, i.e. (9),(10). A possibility of the stator flux amplitude control using the u_{sx} component results from mentioned equations. There appears the factor $\omega_{s\psi}\psi_s$ in the equation (10), which decoupling allows (with constant ψ_s) to control the motor torque (11) using the u_{sy} component.

The schematic diagram of the DTC-SVM is presented in Fig. 1.

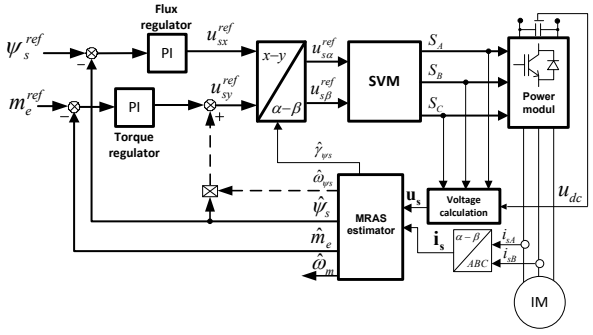

Fig.1. Schematic diagram of the DTC-SVM structure

Reference stator voltage vector components (u_{sx}, u_{sy}) are transformed into the stationary α–β coordinate system using estimated stator flux vector angle. These values become the SVM inputs, which then defines the power module transistors on/off signals S_A, S_B, S_C. The control path decoupling is made using the addition of the product of the signals marked with dashed lines. The necessity of the stator flux velocity estimation in the decoupling path complicates the control structure and introduces noises (arising from the calculation of the derivative of the $\gamma_{s\psi}$ and its filtration). That is why in this paper, just as in the majority of other practical solutions [2], this mechanism is not taken into consideration – the PI torque regulator compensates mention effect effectively.

Field weakening algorithm

Traction drives usually operate with speeds significantly bigger than nominal one, so the control algorithm requires the suitable field weakening strategy. The most frequently applied method of the FW control adjusts the excitation level of the machine by feed-forward control in inverse proportion to the mechanical speed of the motor. This strategy does not take into account the current and voltage limits of the drive system. Thus in the last twenty years renewed interest in the optimal methods for the FW control of IMs [10], [11]. For rotor-flux orientation it was shown that the classical FW method of selecting the flux-producing current component proportional to the rotor speed inverse, yields too large current value, and a maximum torque is not achieved [11]. In the 2000s, several improved techniques have been proposed [12], [13], which take into account current and voltage limits. Maximal allowable voltage of the drive system depends on output voltage u_{dc} of the AC/DC converter and used modulation strategy of the voltage inverter. When the Space Vector Modulation (SVM) with overmodulation strategy is used, this maximal allowable voltage is:

$$u_{\max} = \frac{2}{\pi} u_{dc} \tag{16}$$

Field weakening algorithm, which takes into account his allowable voltage value and maximal stator current value, is

determined in field coordinate system oriented according with the rotor flux vector. According to the basic electrical drive theory [14], three different regions of the drive operation exist, which are shown in Fig. 2.

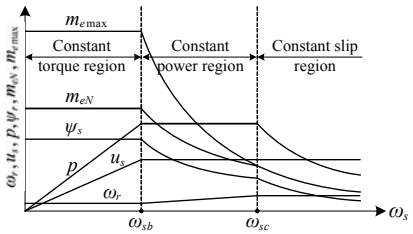

Fig. 2. Operation regions of the drive system (p – power, m_{emax} – maximal (critical) torque, ω_r – slip pulsation).

In the first region – of constant torque, drive system works with constant maximal electromagnetic torque and constant nominal magnitude of the stator flux. In two next regions of constant power and constant slip (two field weakening regions), change of the reference value of stator flux is required. It can be calculated according to the reference value of the rotor flux magnitude, according to [2]:

$$\psi_s^{ref} = \sqrt{\left(\frac{x_s}{x_r}\psi_r^{ref}\right)^2 + \left(\sigma x_s\right)^2\left(\frac{x_r}{x_M}\frac{m_e^{ref}}{\psi_r^{ref}}\right)} \tag{17}$$

$$\psi_r^{ref} = x_M i_{sx}^{ref} \tag{18}$$

The constant power region – 1st FW region starts, when the synchronous speed is bigger than base speed [13], [15]:

$$\omega_s > \omega_{sb},\ \ \omega_{sb} = \frac{u_{\max}}{x_s\sqrt{i_{sxN}^2\left(1-\sigma^2\right)+\sigma^2 i_{\max}^2}} \tag{19}$$

In this region the reference value of the torque component of the stator current vector is equal:

$$i_{sx}^{ref} = \frac{\sqrt{u_{\max}^2 - \omega_s^2 x_s^2 \sigma^2 i_{\max}^2}}{\omega_s x_s\sqrt{1-\sigma^2}} \tag{20}$$

The constant slip region – 2nd FW region starts, when the synchronous speed is bigger than critical speed:

$$\omega_s > \omega_{sc},\quad \omega_{sc} = \frac{u_{\max}\sqrt{2\left(\sigma^2+1\right)}}{2\sigma x_s i_{\max}} \tag{21}$$

In this region the limitation of the stator current will be determined by the maximal allowable value of the stator voltage. Thus magnetizing current component i_{sx} is calculated as follows:

$$i_{sx}^{ref} = \frac{u_{\max}}{\sqrt{2}\omega_s x_s} \tag{22}$$

Estimation of the induction motor speed

Speed estimation can be used in traction drives to ensure the operational reliability in case of the speed encoder failure. In this case simple, but simultaneously robust over disturbances (including parameter disturbances appearing during the traction drive operation within wide range of temperatures) estimator must be used. Model Reference Adaptive System estimators [7] can be ranked as ones of them. These estimators are considered in this paper. Two different solutions will be compared, first of them MRAS^{CC} [5], and another one utilizing the sliding mode theory, SM-MRAS [6]. In these both estimators the rotor flux is estimated using the following formula:

$$T_N\frac{d\hat{\boldsymbol{\psi}}_{\mathbf{r}}}{dt} = -\frac{r_r}{x_r}\hat{\boldsymbol{\psi}}_{\mathbf{r}} + \frac{x_M r_r}{x_r}\mathbf{i}_{\mathbf{s}} + j\hat{\omega}_m\hat{\boldsymbol{\psi}}_{\mathbf{r}} \tag{23}$$

Stator current vector is estimated as follows:

$$T_N\frac{d\hat{\mathbf{i}}_{\mathbf{s}}}{dt} = \frac{1}{x_s\sigma}\left(u_s - r_s\hat{\mathbf{i}}_{\mathbf{s}} - \frac{r_r x_M^2}{x_r^2}\hat{\mathbf{i}}_{\mathbf{s}} + \frac{x_M}{x_r}\frac{r_r}{x_r}\hat{\boldsymbol{\psi}}_{\mathbf{r}} - j\frac{x_M}{x_r}\hat{\omega}_m\hat{\boldsymbol{\psi}}_{\mathbf{r}}\right) \tag{24}$$

Used in both above equations estimated speed is calculated as:

$$\hat{\omega}_m = h\left(s_\omega\right) \tag{25}$$

where: $s_\omega = \left(\hat{i}_{s\beta} - i_{s\beta}\right)\hat{\psi}_{r\alpha} - \left(\hat{i}_{s\alpha} - i_{s\alpha}\right)\hat{\psi}_{r\beta}$.

The $h(s_\omega)$ function defines the adaptation mechanism, and simultaneously the type of the estimator. In case of the MRAS^{CC} estimator this function becomes:

$$h\left(s_\omega\right) = \left(k_P + k_I\frac{1}{p}\right)s_\omega \tag{26}$$

where: p – Laplace operator, while in case of the SM-MRAS estimator:

$$h\left(s_\omega\right) = k_\omega\ \mathrm{sign}\left(s_\omega\right) \tag{27}$$

where parameters k_p, k_I, k_ω=const.

The schematic diagram, showing the different between presented estimators, is shown in the Fig. 3.

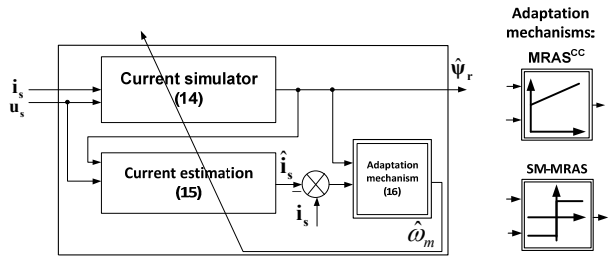

Fig. 3. Schematic diagram of the analysed speed estimators

Since the sign function generates the high frequency signal, filtration of the signal obtained with (28) is necessary. During the tests the simplest low-pass filter was used, i.e. a system with a transfer function of a first order inertial term:

$$\frac{\hat{\omega}_{m,fil}(p)}{\hat{\omega}_m(p)} = \frac{1}{T_f p + 1} \tag{28}$$

where T_f – the filter time constant.

Results of simulation tests

Analysis of the performance of the described sensorless DTC-SVM drive with the described optima FW algorithms been realized using simulation tests in Matlab/Simulink.

In the Fig. 4 simulation transients of the drive system behavior in the 1st FW region are demonstrated. It can be seen that electromagnetic torque (Fig. 4d) and stator flux (Fig. 4e) are controlled ideally, estimated values reach reference values very fast. The motor speed, which results from the forced motor torque, changes according to transient shown in Fig. 4a. The estimated speed follows the

actual speed and the speed estimation error is almost negligible (Fig. 4c). In the analyzed 1st FW region, the synchronous speed of the motor takes values between base and critical speed (see (25) and (27), Fig. 4b). Under simulation tests the constant value of the DC bus voltage was assumed (Fig. 4f).

Transients of the drive system behavior in the 2nd FW region are demonstrated in Fig. 5. Such operation under maximal allowable stator voltage is characterized by really high motor speed (Fig. 5a) and very low torque (Fig. 5d). As in previous case, the motor torque and flux are controlled fast during transients (Fig. 5e, e) and motor speed is estimated with negligible error (Fig. 5c), but a little bigger than in case of Fig. 4c.

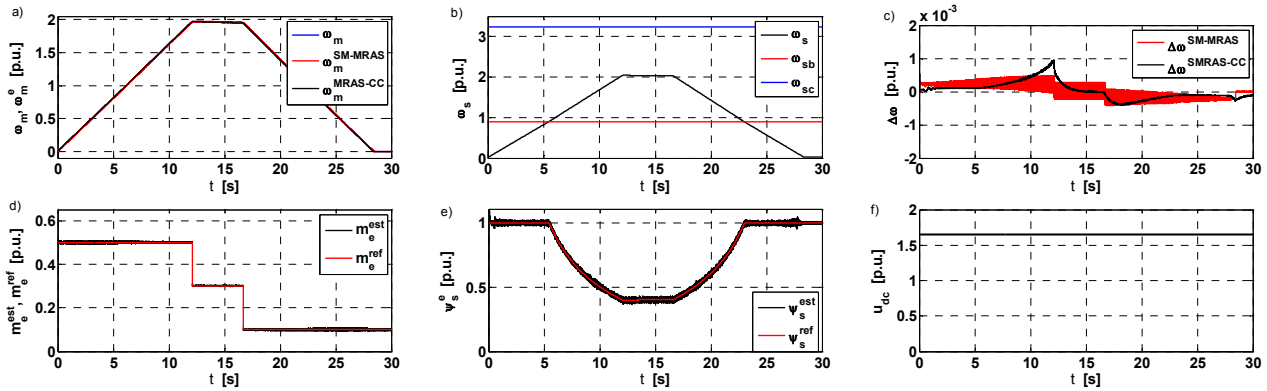

Fig.4. State variable transients of the induction motor drive with DTC-SVM and optimal field weakening strategy, drive operates in 1st FW region: a) Real and estimated speed, b) synchronous, base and critical speed, c) speed estimation error, d) reference and estimated torque, e) reference and estimated stator flux, f) DC input voltage of the inverter

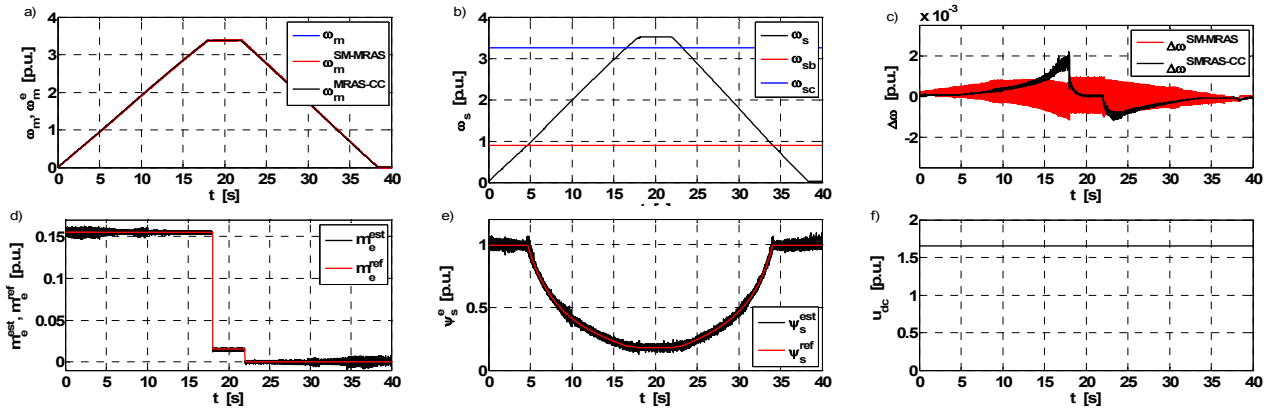

Fig.5. State variable transients of the induction motor drive with DTC-SVM and optimal field weakening strategy, drive operates in the 2nd FW region: a) real and estimated speed, b) synchronous, base and critical speed, c) speed estimation error, d) reference and estimated torque, e) reference and estimated stator flux, f) DC input voltage of the inverter

Results of experimental tests

The analyzed drive system has been tested in the experimental set-up composed of the traction IM of 50 kW (fed from the voltage source inverter (VSI)) and a loading machine (second IM supplied from an AC inverter, with active generation of the loading torque). The speed and position of the drive are measured by the incremental encoders (5000 imp./rev.), only for comparison with the estimated speed in the sensorless drive system (Fig. 6a).

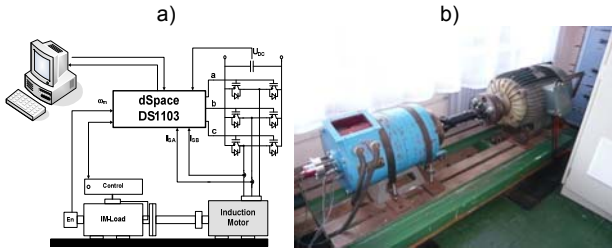

Fig.6. The photo of the 50 kW traction drive system (a) and schematic diagram of the laboratory test bench (b)

The control and estimation algorithms as well as measurement data acquisition have been realized using digital signal processor card DS 1103 (Fig. 6b).

In Fig. 7 the experimental transients of the drive system behavior in the wide range of the motor torque and speed changes are demonstrated, including FW region with the described optimal algorithm. The measured (only for comparison) and estimated motor speed (using both described speed estimators) are presented in Fig. 7a. It can be seen that the estimation error is negligible and the speed was estimated perfectly also in the real drive system. Additionally, the influence of the adaptation function $h(s_\omega)$ of the SM-MRAS speed estimator on the speed estimation error is presented in Fig. 7c. The estimation error of the SM-MRAS estimator is slightly smaller than in a case of MRAS^{CC} estimator. The drive system operates in the 1st FW region between the base and critical speed, as it is shown in Fig. 7b. These pulsations change according to the changeable voltage in the |DC bus circuit (Fig. 7f, Eq. (25) and Eq, (27)). The stator flux magnitude (Fig. 7e) and motor torque (Fig. 7d) follow their reference values.

The drive system works with the load torque close to 50% of the nominal value, with speed over twice nominal one. It is possible due to an active FW algorithm, which cause the

decreasing of the stator flux value depending on the allowable DC bus voltage. Simultaneously the maximal possible motor torque is generated, which is close to (30÷40)% bigger than in a case of classical $1/\omega_{ref}$ FW algorithm.

Unfortunately the 2nd FW region could not be tested experimentally, due to a mechanical limitations of the motors in laboratory set-up.

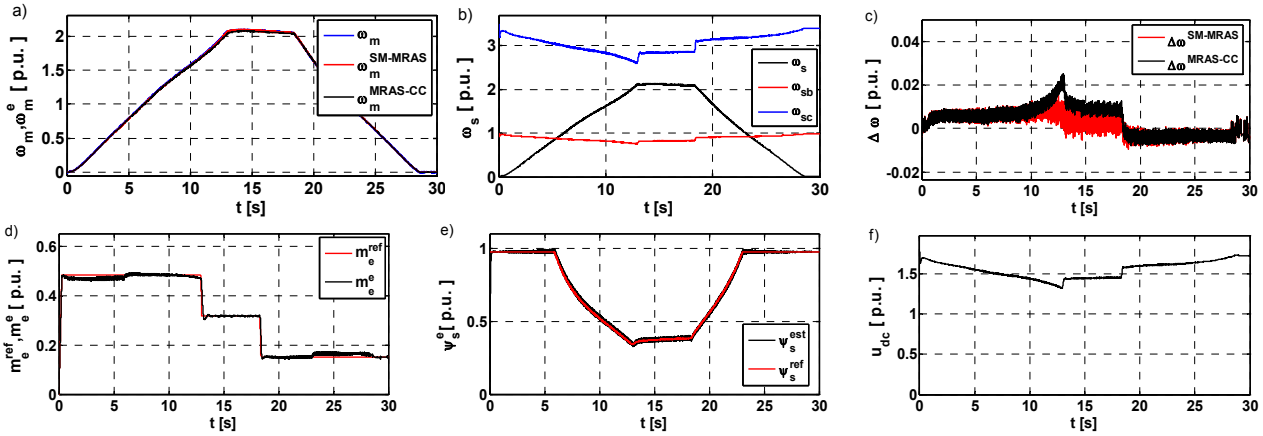

Fig. 7. Experimental transients of the state variables of the induction motor drive with DTC-SVM and optimal field weakening strategy, drive operates in 1st FW region: a) Real and estimated speed, b) synchronous, base and critical speed, c) speed estimation error, d) reference and estimated torque, e) reference and estimated stator flux, f) DC input voltage of the inverter

Conclusions

The sensorless DTC-SVM induction motor drive with optimal field weakening algorithm was analyzed in this paper. The applied FW algorithm takes into account the current limit and voltage limit, which result from the winding temperature limitation and maximal allowable voltage of the DC bus, respectively.

The analyzed drive system has been tested in simulation and experimentally for the 50 kW induction motor drive.

As it has been shown in the paper, the maximal speed obtained in the experimental set-up was more than twice nominal one, with very good performance of the torque and stator flux control. The tested speed estimators, like SM-MRAS and MRAS^{CC} ensured the proper speed estimation quality in the whole tested range and in all operation condition of the drive system.

Due to the application of the described FW algorithm, the allowable voltage of the AC/DC converter has been fully utilized. It was shown that even under changes of the DC bus voltage in the real drive system, the optimal FW algorithm adapts the stator flux properly and required motor torque is generated rapidly, according to its reference value.

Acknowledgements

This research work was supported by the National Centre for Research and Development, Poland, under Grant NR01000106/2009 (2009–2012)

REFERENCES

[1] Orłowska-Kowalska T., *Sensorless induction motor drives*, Wrocław University of Technology Press, Wroclaw, Poland (2003)

[2] Buja G. S., Kazmierkowski M. P., Direct torque control of PWM inverter-fed AC motors - a survey, *IEEE Trans. Ind. Electronics*, 51 (2004), n.4, 744–757.

[3] Tamai S., Sugimoto H., Yano M., Speed sensor-less vector control of induction motor with model reference adaptive system, *IEEE-IAS Annual Meeting*, (1987), 189–195.

[4] Schauder C., Adaptive Speed Identification for Vector Control of Induction-Motors without Rotational Transducers, *IEEE Trans. Ind. Appl.*, 28 (1992), n.5, 1054–1061.

[5] Orłowska-Kowalska T., Dybkowski M., Stator-Current-Based MRAS Estimator for a Wide Range Speed-Sensorless Induction-Motor Drive, *IEEE Trans. Ind. Electronics*, 57 (2010), n.4, 1296–1308.

[6] Yan Z., Jin C. X., Utkin V. I., Sensorless sliding-mode control of induction motors, *IEEE Trans. Ind. Electronics*, 47 (2000), n.6, 2000, 1286–1297.

[7] Tarchała G., Orłowska-Kowalska T., Dybkowski M., MRAS-Type Speed and Flux Estimator with Additional Adaptation Mechanism for the Induction Motor Drive, *Trans. Electrical Engineering.*, 1 (2012), n. 1, 7–12.

[8] Orłowska-Kowalska T., Dybkowski M., Tarchała G., Analysis of chosen speed estimators in induction motor drives – part I – mathematical models, *Scientific Works of the Institute of Electrical Machines, Drives and Measurements of Wroclaw Univ. of Technology, No. 64, ser. Studies and Materials, No. 30,* (2010), 151–161 (in Polish).

[9] Dybkowski M., Orłowska-Kowalska T., Tarchała G., Analysis of chosen speed estimators in induction motor drives – part II – test results, *Scientific Works of the Inst. of Electrical Machines, Drives and Measurements of WUT, No. 64, ser. Studies and Materials, No. 30,* (2010), 162–175 (in Polish).

[10] Kim J.M., Sul S.K., Maximum torque control of an induction machine in the field weakening region, *IEEE Trans. Ind. Applicat.,* 31 (1995), n.4, 787-794.

[11] Xu X., Novotny D.W., Selection of the flux reference for induction machine drives in the field weakening region, *IEEE Trans. Ind. Application,* 28 (1992), n.6, 1353-1358.

[12] Harnefors L., Pietilainen K., Gertmar L., Torque-maximizing field-weakening control: design, analysis, and parameter selection, *IEEE Trans. Ind. Electronics*, 48 (2001), n.1, 161-168.

[13] Gallegos-Lopez G., Gunawan F. S., Walters J. E., Current control of induction machines in the field-weakened 9region, *IEEE Trans. Ind. Appl.*, 43 (2007), n.4, 981–989.

[14] Kazmierkowski M. P., Tunia H., *Automatic Control of Converter-Fed Drives*, Elsevier Amsterdam-London-New York-Tokyo (1994).

[15] Nguyen Thac K., Orłowska-Kowalska T., Comparative Analysis of Chosen Field Weakening Methods for the Space Vector Modulated - Direct Torque Controlled Drive System, *Scientific Works of the Inst. of Electrical Machines, Drives and Measurements of Wroclaw Univ. of Technol., No. 65, ser. Studies and Materials, No. 31,* (2011), 267-280

***Authors**: mgr inż. Grzegorz Tarchała*
prof. dr hab. inż. Teresa Orłowska-Kowalska
mgr inż. Khanh Nguyen Thac
dr inż. Mateusz Dybkowski
Politechnika Wrocławska, Instytut Maszyn, Napędów i Pomiarów Elektrycznych, ul. Smoluchowskiego 19, 50-372 Wrocław,
E-mail: teresa.orlowska-kowalska,@pwr.wroc.pl,
grzegorz.tarchala@pwr.wroc.pl, mateusz.dybkowski@pwr.wroc.pl, khanh.nguyen.thac@pwr.wroc.pl